ATTITUDE CONTROL

Attitude control is the field of engineering science that deals with the control of the rotational motion of a rigid body about a reference point (typically the center of mass). Attitude control systems are commonly used in controlling the orientation of spacecraft or aircraft. As a spacecraft orbits the Earth, it may have to move in space in such a way that its antenna always points to a ground station for communication or its on-board telescope keeps pointing to a distant star. A fighter aircraft may be required to turn very fast and maneuver aggressively to shoot down enemy airplanes or to avoid an incoming missile. A civilian airplane may need to keep a constant cruising altitude, to perform a turn without excessive side forces, or to land in bad weather or low visibility. All these tasks are performed with the help of an attitude control system.

An attitude control system is a collection of attitude sensors, actuators, and an attitude control law. The objective of an attitude control system is to acquire information about the orientation of the vehicle from the attitude sensors, process this information through an attitude control law, and generate a series of commands that will change or keep the attitude of the vehicle at a specified orientation. An *attitude control law* is an algorithm (i.e., a series of commands or instructions), which calculates the necessary action to be taken based on the knowledge of the current and anticipated attitude. This algorithm is usually executed on a digital or an analog computer. When the control law simply follows a set of prespecified steps stored in the computer's memory or given to the computer by a human operator we refer to the control algorithm as an *open-loop* control law. If the computer makes its decisions without external intervention, solely on attitude measurements from its sensors, the control law is referred to as *feedback* or *closed-loop* attitude control law.

ATTITUDE CONTROL OF SPACECRAFT

A rigid satellite or spacecraft in orbit offers the most obvious example of a rotating rigid body. Attitude control for spacecraft arises in the process of orienting the spacecraft along a specified, predetermined direction. According to Wertz (1), it consists of two problems—*attitude stabilization,* or maintaining a specific orientation, and *attitude maneuver control,* or, controlling the spacecraft from one attitude orientation to another. Attitude orientation is specified either with respect to an inertial reference frame or with respect to another moving object. For instance, attitude stabilization of a spacecraft with one axis toward the Earth implies a continuously changing orientation with respect to an inertial frame. There are two main methods for spacecraft stabilization: (1) *passive* methods, and (2) *active* methods.

Passive Stabilization

Passive methods require no power consumption or external control. The stabilization is achieved naturally through the physical properties of the motion. Two typical methods of passive stabilization are gravity-gradient stabilization and spin stabilization. *Gravity-gradient stabilization* is based on the natural balancing torque due to the gravity differential at two distinct points of a body at different distances from the center of the Earth. It is a particularly effective way for stabilization of elongated structures at low Earth orbit where the gravity pull of the Earth is stronger. The result of this stabilization method is to keep the long dimension of the structure along the local vertical (the direction to the center of the Earth).

Spin stabilization on the other hand, takes advantage of the natural tendency of the angular momentum vector to remain inertially fixed in the absence of external torques. The term *gyroscopic stiffness* is often used to describe this property of the angular momentum vector. A child's familiar spinning top is based on the same principle. Spin stabilization aims to keep the axis of rotation (spin axis) and the angular momentum vector parallel. This ensures that the spin axis remains inertially fixed. If the spin axis and the angular momentum vector are not parallel, the spacecraft is said to exhibit *nutation,* which manifest itself as a *wobbling* motion. In the presence of damping (i.e., energy dissipation) the vehicle spin axis tends to align itself with the angular momentum axis. In practice *nutation dampers* are used to introduce artificial damping in order to align the spin and the angular momentum axis and thus keep the spin axes constant in inertial space.

Gravity-gradient or spin stabilization cannot be used to control the body about the gravity vector or the spin axis. In addition, it may not always be possible to use spin stabilization. For example, mission requirements may demand that the communications antenna always point toward Earth, or the solar panels point always toward the sun. In this case, it is necessary that the antenna and the solar panels be stationary with respect to an inertial frame. They cannot be part of a continuously spinning satellite. The solution to this problem is the use of *dual spin spacecraft* or *dual spinners,* which consist of two parts, the rotor and the stator. The rotor rotates about its axis and provides the angular momentum necessary for stabilization as with case of the spin-stabilized spacecraft. The stator remains fixed and contains all the scientific instruments that have to remain inertially fixed. Thus, dual-spin spacecraft combine scanning (rotating) and pointing (inertially fixed) instruments in one platform. This clever solution comes at the expense of increased complexity of the spacecraft design and its operation, however.

A *momentum bias* design is very common for dual-spin satellites in low-Earth orbit, in which the rotor is mounted along the normal to the orbit plane. This allows the instruments to scan the Earth. Other common methods of passive stabilization include magnetic torques or use of solar panels.

Active Stabilization

Although simple and cheap, passive stabilization schemes have two main drawbacks: First, they achieve pointing accuracy of the controlled axis only up to a few degrees. Several applications (e.g., communications satellites, space telescopes, etc.) require accuracy of less than a few arc seconds (1 arcsecond = 1/3600 deg). Second, control systems based on passive schemes cannot be used effectively to perform large attitude maneuvers. Reorientation of the spin axis for a spinning spacecraft, for instance, requires excessively large control torques to move the angular momentum vector. Also, gravity-gradient and magnetic torques are limited by the direction of their respective force fields and, in addition, are not strong enough to be used for arbitrary, large angle maneuvers.

Both of the previous problems encountered in the use of passive stabilization schemes can be resolved using active stabilization methods. The most common active control methods incorporate use of gas actuators or momentum wheels. Both can be used to achieve *three-axis stabilization,* that is, active control of the spacecraft orientation about all three axes, as well as *three-axis large angular (slew) maneuvers.*

Gas actuators use a series of gas nozzles distributed (usually in pairs) along the three perpendicular axes of the spacecraft. Gas jets are classified either as hot gas jets (when a chemical reaction is involved) or cold gas jets (when no chemical reaction is present). The gas jets (thrusters) are usually of the on–off type. Continuously varying control profiles can be generated, however, using pulse-width pulse-frequency (PWPF) modulators. These modulators produce a continuously varying control torque by generating a pulse command sequence to the thruster valve by adjusting the pulse width and pulse frequency. The average torque thus produced by the thruster equals the demanded torque input. This will wear out the jet valves in the long run. A better choice for generating continuously varying torques is the use of momentum wheels.

Gas jets achieve stabilization by generating *external torques,* which change the total angular momentum of the spacecraft. Alternatively, flywheels can be used to generate *internal torques* or redistribute the angular momentum between the main vehicle and the wheels. The total angular momentum of the vehicle plus the wheels remains constant in this case. This is akin to a gymnast throwing a somersault. While in the air, the gymnast's angular momentum is constant. The gymnast changes position and rotates in midair by redistributing the angular momentum by extending or contracting the arms, bending at the waist, and so on. Momentum exchange devices (sometimes collectively referred to as momentum wheels) are also preferable for application of continuously varying torques. There are three main types of actuators that use momentum exchange for attitude control.

1. *Reaction wheels* do not rotate under normal conditions. When an angular maneuver is commanded or sensed, the reaction wheel spins in the opposite direction to the sensed or commanded rotation. Thus a reaction wheel provides a torque along the wheel spin axis. A minimum of three reaction wheels is necessary to control the attitude about all three axes.
2. *Momentum wheels* spin at a constant speed under normal conditions, and are used to increase stability about the corresponding axis. A dual-spin spacecraft, for example, is a special case of a spacecraft with a momentum wheel about the axis of symmetry. A minimum of three wheels are necessary to achieve stability about all three axes.
3. *Control moment gyros* (CMG) consist of a single spinning flywheel that is gimballed and free to rotate about two or three perpendicular axes. Contrary to the momentum wheel, the magnitude of the angular velocity vector remains constant. The torque produced is proportional to the change in the direction of the angular momentum vector.

A more complete discussion on the use of momentum wheels in attitude control problems can be found elsewhere (1,2).

Attitude Sensors

As mentioned earlier, an attitude control system requires information about the body orientation. This information is provided by attitude sensors. An attitude sensor actually provides the relative orientation of the spacecraft with respect to a reference vector (e.g., a unit vector in the direction of the Sun, a known star, the Earth, or the Earth's magnetic field). Therefore, three-axis attitude determination requires two or more sensors. The definitive reference for a more in-depth discussion of attitude sensors and actuators and their principles of operation is Wertz (1). This reference also includes a fairly detailed overview of hardware implementation issues.

Sun Sensors. Sun sensors are the most common type of attitude sensor. Their field of view ranges from a few square arc-min (10^{-7} rad^2) to approximately π rad^2 and their resolution ranges from several degrees to less than 1 arc-sec.

Horizon Sensors. Horizon sensors can be used when the spacecraft is in a close orbit around a celestial body. For low-Earth orbiting satellites, for instance, the difference in brightness of Earth's disk from the background darkness of space can be easily detected by a horizon sensor and provides a coarse attitude measurement.

Magnetometers. Magnetometers use Earth's magnetic field to locate the body's orientation. They have poor resolution due to uncertainty of Earth's magnetic field. They work better at low-Earth orbits, where the magnetic field is stronger and better modeled.

Star Sensors. Star sensors provide attitude information of very high accuracy, but they are heavy and expensive. They are usually the choice for deep-space spacecraft where attitude measurements from Sun sensors or near-by celestial objects are either unavailable or inaccurate.

Gyroscopes. Gyroscopes (or simply gyros) use a rapidly spinning mass on a gimbal to sense changes in the spacecraft orientation. The principle of their operation is based on the fact that any change in the angular momentum vector about a certain axis will be sensed as a resulting movement about a perpendicular axis. They are very accurate for limited time intervals, but their measurements may become inaccurate over long periods of time due to drift. In this case, they have to be combined with some other attitude sensor to reset them periodically. Gyroscopes can also be used to get angular velocity measurements; in this case they are called *rate gyros*. Apart from their use in spacecraft, gyroscopes are also used as attitude or angular velocity sensors in aircraft, missiles, or marine vehicles (e.g., submarines).

DYNAMICS OF ROTATING BODIES

The motion of a rigid body in three-dimensional space is determined by the forces and moments acting on the body at each instant of time. There are two main types of general motion of a rigid body: (1) *translational motion,* which typically deals with the velocity and position of the center of mass of the body, and (2) *rotational* or *attitude motion,* which typically deals with the (angular) velocity and (angular) position about the center of mass. The angular position about the center of mass is often referred to as the *attitude* or *orientation* of the body. The choice of the center of mass as the reference point to describe the general body motion is not restrictive, but it has the advantage of allowing the rotation and translation to be treated separately. That is, the translation of the body center of mass does not affect nor is it affected by the rotation of the body about the center of mass.

To understand the two types of motion, consider the example of a spacecraft traveling in space. The spacecraft translates and rotates at the same time. For an observer located on Earth, the spacecraft can be thought of as a single particle, and its trajectory through space is primarily determined by its instantaneous position and velocity. Its orientation with respect to Earth is irrelevant (unless a communication antenna needs to be always pointing toward Earth) or very difficult to observe from such a large distance. On the other hand, as the same observer moves closer and closer to the spacecraft, the orientation of the spacecraft may be very important, and it certainly becomes much more obvious.

Translational motion therefore deals with the motion of *particles,* that is, idealized points with zero dimensions but nonzero mass. Rotational motion, on the other hand, deals with the motion of *rigid bodies,* that is, physical objects with nonzero dimensions and nonzero mass. One can safely think of translation as the macroscopic, or far-away view of the motion of an object and of rotation as the microscopic, or close-by view of the motion.

Dynamics of the Attitude Motion

The dynamic equations of the attitude motion of a rotating body describe the behavior of the angular momentum or the angular velocity vector as a function of the externally applied torques or moments. The basic equation that governs the body behavior under external torques is Euler's equation of motion (2). It states that the rate of change of the angular momentum vector $\boldsymbol{H}$ of the body at every instant is equal to the applied moment $\boldsymbol{M}$

$$\frac{d\boldsymbol{H}}{dt} = \boldsymbol{M} \tag{1}$$

where the angular momentum is defined by

$$\boldsymbol{H} = \int_B \boldsymbol{r} \times \boldsymbol{v}\, dm \tag{2}$$

and the integration extends over the entire body. In Eq. (2) the vector $\boldsymbol{v} = \dot{\boldsymbol{r}}$ denotes the inertial velocity of the mass element dm (see Fig. 1).

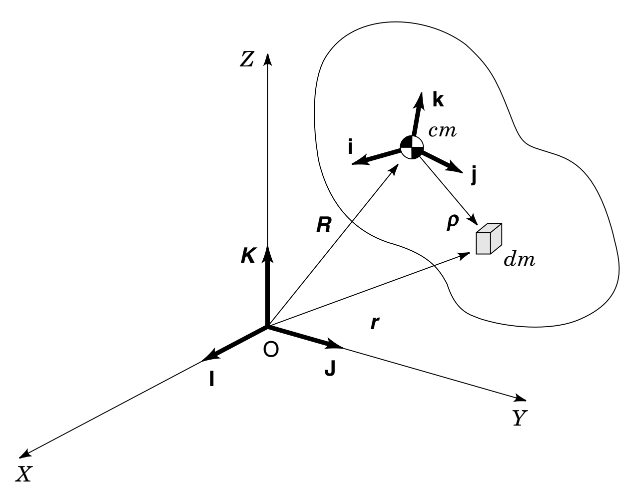

Figure 1. Inertial and body-fixed reference frames. The body-fixed reference frame is located at the center of mass *cm*. The vector **r** denotes the location of the element mass *dm* in the inertial frame and the vector $\boldsymbol{\rho}$ denotes the location of the mass in the body frame.

The time derivative in Eq. (1) must be taken with respect to an inertial reference frame. In addition, in the calculation of $\boldsymbol{H}$ we have a choice of the reference point about which to calculate the moments and the angular momentum. Equation (1) implies that we have chosen either a point fixed in inertial space or the center of mass. The center of mass offers the most convenient and natural choice. In this case, from Fig. 1 we have that the location of the mass element dm is at $\boldsymbol{r} = \boldsymbol{R} + \boldsymbol{\rho}$, where $\boldsymbol{R}$ denotes the location of the center of mass.

Differentiation of a vector $\boldsymbol{V}$, as seen from an inertial frame, is related to differentiation as seen in a moving (body) frame through the relationship

$$\left.\frac{d\boldsymbol{V}}{dt}\right|_{\mathrm{I}} = \left.\frac{d\boldsymbol{V}}{dt}\right|_{\mathrm{B}} + \boldsymbol{\omega} \times \boldsymbol{V} \tag{3}$$

where $\boldsymbol{\omega}$ is the angular velocity of the moving frame. The velocity of the mass element dm is thus given by

$$\boldsymbol{v} = \dot{\boldsymbol{R}} + \boldsymbol{\omega} \times \boldsymbol{\rho} \tag{4}$$

Subsequently, the angular momentum vector is given by

$$\boldsymbol{H} = \int_{\mathrm{B}} \boldsymbol{\rho} \times \dot{\boldsymbol{R}}\, dm + \int_{\mathrm{B}} \boldsymbol{\rho} \times (\boldsymbol{\omega} \times \boldsymbol{\rho})\, dm \tag{5}$$

The first integral in the previous expression vanishes, because the origin is at the center of mass

$$\int_{\mathrm{B}} \boldsymbol{\rho}\, dm = 0 \tag{6}$$

The angular momentum vector with respect to the center of mass is thus

$$\boldsymbol{H} = \int_{\mathrm{B}} \boldsymbol{\rho} \times (\boldsymbol{\omega} \times \boldsymbol{\rho})\, dm \tag{7}$$

Since the position vector $\boldsymbol{\rho}$ changes with time in an inertial frame, it is beneficial to choose a reference frame fixed in the body, since in this case the mass distribution does not change.

Therefore, choosing a reference frame fixed in the body and located at the center of mass, we can express $\boldsymbol{\omega}$ and $\boldsymbol{\rho}$ in this body-fixed frame as

$$\boldsymbol{\omega} = \omega_{\mathrm{x}}\mathbf{i} + \omega_{\mathrm{y}}\mathbf{j} + \omega_{\mathrm{z}}\mathbf{k}, \quad \boldsymbol{\rho} = x\mathbf{i} + y\mathbf{j} + z\mathbf{k} \tag{8}$$

Then Eq. (7) yields

$$\boldsymbol{H} = J\boldsymbol{\omega} \tag{9}$$

where J is the *moment-of-inertia* matrix and is given by

$$J = \begin{bmatrix} J_x & -J_{xy} & -J_{xz} \\ -J_{xy} & J_y & -J_{yz} \\ -J_{xz} & -J_{yz} & J_z \end{bmatrix} \tag{10}$$

where

$$\begin{aligned} J_{\mathrm{x}} &= \int_{\mathrm{B}} (y^2 + z^2)\, dm, & J_{\mathrm{xy}} &= \int_{\mathrm{B}} xy\, dm \\ J_{\mathrm{y}} &= \int_{\mathrm{B}} (x^2 + z^2)\, dm, & J_{\mathrm{xz}} &= \int_{\mathrm{B}} xz\, dm \\ J_{\mathrm{z}} &= \int_{\mathrm{B}} (x^2 + y^2)\, dm, & J_{\mathrm{yz}} &= \int_{\mathrm{B}} yz\, dm \end{aligned} \tag{11}$$

The moment-of-inertia matrix depends on the shape of the body and the manner in which its mass is distributed. The larger the moments of inertia the greater resistance the body will have to rotation.

When using Eq. (3) and recalling that in a body-fixed frame the inertia matrix is constant, it follows that Eq. (1) can be written as

$$J\dot{\boldsymbol{\omega}} + \boldsymbol{\omega} \times J\boldsymbol{\omega} = \boldsymbol{M} \tag{12}$$

The inertia matrix J, also called the *inertia tensor,* is symmetric and positive definite. One can therefore choose a reference frame such that the matrix J is diagonal. This particular choice of body-fixed axes is called the axes of *principal moments of inertia.* The directions of these axes are exactly those determined by the eigenvectors of the matrix J.

The components of Eq. (12) resolved along the principal axes are given by

$$\begin{aligned} J_{\mathrm{x}}\dot{\omega}_{\mathrm{x}} &= (J_{\mathrm{y}} - J_{\mathrm{z}})\omega_{\mathrm{y}}\omega_{\mathrm{z}} + M_{\mathrm{x}} \\ J_{\mathrm{y}}\dot{\omega}_{\mathrm{y}} &= (J_{\mathrm{z}} - J_{\mathrm{x}})\omega_{\mathrm{z}}\omega_{\mathrm{y}} + M_{\mathrm{z}} \\ J_{\mathrm{z}}\dot{\omega}_{\mathrm{z}} &= (J_{\mathrm{x}} - J_{\mathrm{y}})\omega_{\mathrm{x}}\omega_{\mathrm{y}} + M_{\mathrm{z}} \end{aligned} \tag{13}$$

where $J_{\mathrm{x}}, J_{\mathrm{y}}, J_{\mathrm{z}}$ are the three principal moments of inertia (the eigenvalues of the matrix J), $\omega_{\mathrm{x}}, \omega_{\mathrm{y}}, \omega_{\mathrm{z}}$ are the components of the angular velocity vector along the principal axes, as in Eq. (8), and $M_{\mathrm{x}}, M_{\mathrm{y}}, M_{\mathrm{z}}$ are the components of the applied moment along the same set of axes, i.e., $\boldsymbol{M} = M_{\mathrm{x}}\mathbf{i} + M_{\mathrm{y}}\mathbf{j} + M_{\mathrm{z}}\mathbf{k}$.

Equation (12) or Eq. (13) is the starting point for most attitude control problems.

Kinematics of the Attitude Motion

The solution of Eq. (13) provides the instantaneous angular velocity of the body about its center of mass. It does not capture the instantaneous orientation of the body with respect to, say, the inertial reference frame. In particular, integration of the angular velocity vector ω does not, in general, give any useful information about the orientation of the body. The orientation of the body is completely determined if we know the orientation of the body-fixed frame with respect to the inertial reference frame, used in deriving Eq. (13). The *rotation matrix* R between the body-fixed and the inertial reference frames is used to completely describe the body orientation. The rotation matrix is a 3×3 matrix having as columns the components of the unit vectors of the inertial frame expressed in terms of the unit vectors of the body-fixed frame.

In other words, $\mathbf{i}, \mathbf{j}, \mathbf{k}$ denote the unit vectors of the body frame and $\mathbf{I}, \mathbf{J}, \mathbf{K}$ denote the unit vectors in the inertial frame, a vector $\boldsymbol{V}$ having coordinates $(V_{\mathrm{x}}, V_{\mathrm{y}}, V_{\mathrm{z}})$ and $(V_{\mathrm{X}}, V_{\mathrm{Y}}, V_{\mathrm{Z}})$ with respect to the body-fixed and inertial frames, respectively, can be written as

$$\boldsymbol{V} = V_x\mathbf{i} + V_y\mathbf{j} + V_z\mathbf{k} = V_X\mathbf{I} + V_Y\mathbf{J} + V_Z\mathbf{K} \tag{14}$$

The matrix R establishes the following relation between the *coordinates* of $\boldsymbol{V}$ in the two reference frames

$$\begin{bmatrix} V_x \\ V_y \\ V_z \end{bmatrix}_B = R \begin{bmatrix} V_X \\ V_Y \\ V_Z \end{bmatrix}_I \tag{15}$$

If $\boldsymbol{\omega} = \omega_x\mathbf{i} + \omega_y\mathbf{j} + \omega_z\mathbf{k}$ denotes the angular velocity of the body frame with respect to the inertial frame (expressed in the body frame coordinates), the differential equation satisfied by R is given by (3,4)

$$\frac{dR}{dt} = S(\omega)R \tag{16}$$

where $S(\omega)$ is the skew-symmetric matrix ($S = -S^T$)

$$S(\omega) = \begin{bmatrix} 0 & \omega_z & -\omega_y \\ -\omega_z & 0 & \omega_x \\ \omega_y & -\omega_x & 0 \end{bmatrix} \tag{17}$$

It can be shown that the matrix R is *orthogonal,* that is, it satisfies

$$RR^T = R^TR = I \tag{18}$$

and it is also proper, that is, its determinant is +1. Equation (16) can also be used to calculate the angular velocity if the rate of change of R is known

$$S(\omega) = \dot{R}R^T \tag{19}$$

We can use Eq. (16) to find the orientation of the body at any instant of time if the corresponding angular velocity vector $\boldsymbol{\omega}$ of the body is known. In particular, the matrix differential equation in Eq. (16) can be integrated from the known initial attitude of the body to *propagate* the attitude for all future times. This process will require the integration of the nine linear but time-varying differential equations for the elements of the matrix R in order to obtain $R(t)$ at each time t. Careful examination of the matrix R, however, reveals that the nine elements of this matrix are not independent from each other, since the matrix R must necessarily satisfy the constraints in Eq. (18). An alternative approach to solving Eq. (16) is to parameterize the matrix R in terms of some other variables and then use the differential equations of these variables in order to propagate the attitude history.

Euler Angles. The minimum number of parameters that can be used to parameterize all nine elements of R is three. [Notice that Eq. (18) imposes six independent constraints among the elements of R.] The Euler angles are the most commonly used three-dimensional parameterization of the rotation matrix R. They have the advantage that they are amenable to physical interpretation and can be easily visualized.

Using the Euler angles we can describe the final orientation of the body-axis frame by three successive elementary rotations. Several definitions of the Euler angles are possible, depending on the choice of the axes of rotations and the particular order in which the rotations are performed. In fact, there are 12 different possible choices of Euler angle sets. These sets have been discussed in great detail elsewhere (3). One of the most common choices in aircraft and spacecraft attitude control problems is the (3-2-1) Euler angle sequence. According to this set of Euler angles, the orientation of the body-fixed reference frame with respect to the inertial reference frame is described by a sequence of the following three elementary rotations:

1. First rotate the inertial reference frame about its Z axis through an angle ψ to the new axes $x' - y' - z'$.
2. Then rotate about the y' axis by an angle θ to the new axes $x'' - y'' - z''$.
3. Finally rotate about the x'' axis by an angle ϕ to the final body-axes x, y, z.

This sequence of rotations that takes the inertial frame to coincide with the body frame after three rotations is depicted in Fig. 2. Note that the order of rotations is very important. The angles ϕ, θ, and ψ are called the roll, pitch, and yaw angles.

The elementary rotations of a reference frame about the axes x, y, and z are given, respectively, by

$$\begin{aligned} R_x(\phi) &= \begin{bmatrix} 1 & 0 & 0 \\ 0 & \cos\phi & \sin\phi \\ 0 & -\sin\phi & \cos\phi \end{bmatrix} \\ R_y(\theta) &= \begin{bmatrix} \cos\theta & 0 & -\sin\theta \\ 0 & 1 & 0 \\ \sin\theta & 0 & \cos\theta \end{bmatrix} \\ R_z(\psi) &= \begin{bmatrix} \cos\psi & \sin\psi & 0 \\ -\sin\psi & \cos\psi & 0 \\ 0 & 0 & 1 \end{bmatrix} \end{aligned} \tag{20}$$

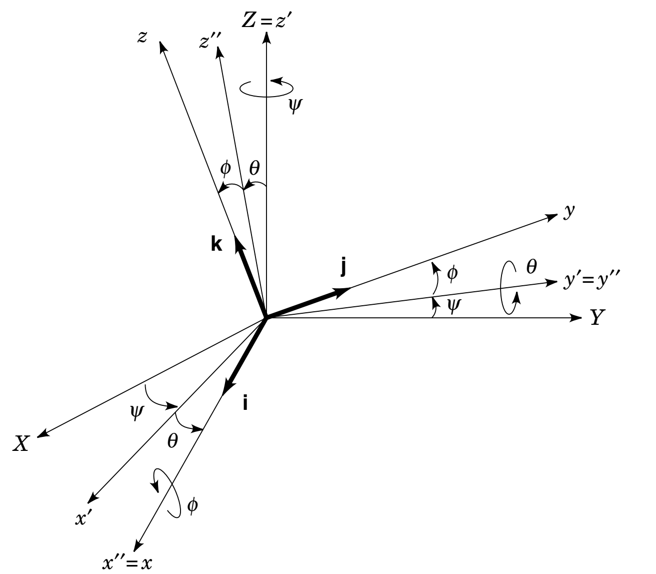

Figure 2. Euler angle sequence (3-2-1). We align the inertial and body frames by first rotating with an angle ψ about the z axis, then rotating with an angle θ about the new y axis, and finally rotating with an angle ϕ about the x axis.

The rotation matrix in terms of the (3-2-1) Euler angles can thus be expressed in terms of the three previous elementary rotations by

$$R(\psi,\theta,\phi) = R_x(\phi)R_y(\theta)R_z(\psi) \tag{21}$$

and thus

$$R(\psi,\theta,\phi) = \begin{bmatrix} \cos\psi\cos\theta & \sin\psi\cos\theta & -\sin\theta \\ -\sin\psi\cos\phi + \cos\psi\sin\theta\sin\phi & \cos\psi\cos\phi + \sin\psi\sin\theta\sin\phi & \cos\theta\sin\phi \\ \sin\psi\sin\phi + \cos\psi\sin\theta\cos\phi & -\cos\psi\sin\phi + \sin\psi\sin\theta\cos\phi & \cos\theta\cos\phi \end{bmatrix} \tag{22}$$

The components of the angular velocity vector in the body-frame are given in terms of the rates of these Euler angles by

$$\begin{aligned} \omega_x &= -\dot\psi\sin\theta + \dot\phi \\ \omega_y &= \dot\psi\cos\theta\sin\phi + \dot\theta\cos\phi \\ \omega_z &= \dot\psi\cos\theta\cos\phi - \dot\theta\sin\phi \end{aligned} \tag{23}$$

Conversely, we can solve the previous equations and express the rates of the Euler angles in terms of the angular velocity components in the body-frame

$$\begin{aligned} \dot\phi &= \omega_x + \omega_y\tan\theta\sin\phi + \omega_z\tan\theta\cos\phi \\ \dot\theta &= \omega_y\cos\phi - \omega_z\sin\phi \\ \dot\psi &= \omega_y\sec\theta\sin\phi + \omega_z\sec\theta\cos\phi \end{aligned} \tag{24}$$

The previous equation indicates that there is a singularity when $\theta = \pm\pi/2$. This singularity does not allow for a global parameterization of the attitude using the Euler angles. The previous (3-2-1) Euler sequence, for example, is defined only for $-\pi \le \phi \le \pi$, $-\pi/2 < \theta < \pi/2$, and $-\pi \le \psi \le \pi$. Other three-dimensional parameterizations include the Cayley-Rodrigues parameters and the modified Rodrigues parameters (4). However, the singularity problem is always present, when using a three-dimensional parameterization of the rotation matrix R (5). Higher order parameterizations need to be used to avoid singularities.

Euler Parameters (Quaternions). A four-dimensional parameterization of the attitude kinematics that does not have any singularities is given by the Euler parameters. The Euler parameters are defined via Euler's theorem, which can be stated as follows (6):

> The most general displacement of a rigid body with one point fixed is equivalent to a single rotation about some axis through that point.

The corresponding axis is called the *eigenaxis of rotation,* and and the corresponding angle is called the *principal angle.* If the eigenaxis unit vector is $\mathbf{e} = e_1\mathbf{i} + e_2\mathbf{j} + e_3\mathbf{k}$ and the principal angle is Φ, the Euler parameters are defined by

$$q_0 = \cos\frac{\Phi}{2}, \quad q_i = e_i\sin\frac{\Phi}{2}, \quad i = 1,2,3 \tag{25}$$

The Euler parameters satisfy the constraint

$$q_0^2 + q_1^2 + q_2^2 + q_3^2 = 1 \tag{26}$$

The quantity

$$q = q_0 + q_1\mathbf{i} + q_2\mathbf{j} + q_3\mathbf{k} \tag{27}$$

defined from the Euler parameters is called the *quaternion* (4,7). It should be pointed out that there is often a confusion in the literature about this term. With a slight abuse of terminology, many authors refer to the Euler parameters q_0, q_1, q_2, q_3 as the quaternion although, strictly speaking, this is incorrect.

The rotation matrix in terms of the Euler parameters is given by

$$R(q_0,q_1,q_2,q_3) = \begin{bmatrix} q_0^2+q_1^2-q_2^2-q_3^2 & 2(q_1q_2+q_0q_3) & 2(q_1q_3-q_0q_2) \\ 2(q_1q_2-q_0q_3) & q_0^2-q_1^2+q_2^2-q_3^2 & 2(q_2q_3+q_0q_1) \\ 2(q_1q_3+q_0q_2) & 2(q_2q_3-q_0q_1) & q_0^2-q_1^2-q_2^2+q_3^2 \end{bmatrix} \tag{28}$$

and the corresponding kinematic equations are given by

$$\begin{bmatrix} \dot q_0 \\ \dot q_1 \\ \dot q_2 \\ \dot q_3 \end{bmatrix} = \frac{1}{2}\begin{bmatrix} 0 & -\omega_x & -\omega_y & -\omega_z \\ \omega_x & 0 & \omega_z & -\omega_y \\ \omega_y & -\omega_z & 0 & \omega_x \\ \omega_z & \omega_y & -\omega_x & 0 \end{bmatrix}\begin{bmatrix} q_0 \\ q_1 \\ q_2 \\ q_3 \end{bmatrix} \tag{29}$$

These equations are linear and do not involve any trigonometric functions as the corresponding kinematic equations in terms of the Euler angles. Integration of these equations to obtain attitude information can thus be performed very fast on a computer. In addition, the attitude description in terms of q_0, q_1, q_2, q_3 is global and nonsingular. For these reasons the Euler parameters have increasingly gained popularity in many attitude-control applications.

The main disadvantage when using the Euler parameters is that they are difficult to visualize. The orientation needs to be transformed to an Euler angle sequence if they are to be meaningful, for example to a pilot or an engineer. The Eulerian angles (ϕ, θ, ψ) in terms of the Euler parameters can be computed, for example, from

$$\begin{aligned} \sin\theta &= 2(q_1q_3 - q_0q_2) \\ \tan\psi &= \frac{2(q_1q_2+q_0q_3)}{q_0^2+q_1^2-q_2^2-q_3^2} \\ \tan\phi &= \frac{2(q_2q_3+q_0q_1)}{q_0^2-q_1^2-q_2^2+q_3^2} \end{aligned}$$

The Euler parameters are related to the (3-2-1) Euler angles by

$$\begin{aligned} q_0 &= \cos(\phi/2)\cos(\theta/2)\cos(\phi/2) + \sin(\phi/2)\sin(\theta/2)\sin(\psi/2) \\ q_1 &= \sin(\phi/2)\cos(\theta/2)\cos(\psi/2) - \cos(\phi/2)\sin(\theta/2)\sin(\psi/2) \\ q_2 &= \cos(\phi/2)\sin(\theta/2)\cos(\psi/2) + \sin(\phi/2)\cos(\theta/2)\sin(\psi/2) \\ q_3 &= \cos(\phi/2)\cos(\theta/2)\sin(\psi/2) - \sin(\phi/2)\sin(\theta/2)\cos(\psi/2) \end{aligned} \tag{30}$$

Careful examination of Eq. (28) shows that both a given set of values of q_0, q_1, q_2, q_3, as well as and their negatives give the same rotation matrix R. Every orientation corresponds to two different sets of Euler parameters. This slight ambiguity has no significant effect in applications, however.

STABILITY OF THE TORQUE-FREE MOTION

When no external forces or moments act on the body, it rotates freely about its center of mass. Its motion is called torque-free (2). If we perturb this torque-free motion slightly by exerting, say, a small impulse, the subsequent motion may or may not be similar to the motion before the impulse was applied. If the ensuing motion is similar or close to the motion before the impulse, we say that the motion of the body is *stable*. If, on the other hand, the motion after the impulse departs significantly from the original one, we say that the motion of the body is *unstable*.

The stability of a torque-free rigid body can be analyzed by setting $M_x = M_y = M_z = 0$ in Eq. (13)

$$\begin{aligned} J_x\dot{\omega}_x &= (J_y - J_z)\omega_y\omega_z \\ J_y\dot{\omega}_y &= (J_z - J_x)\omega_z\omega_x \\ J_z\dot{\omega}_z &= (J_x - J_y)\omega_x\omega_y \end{aligned} \tag{31}$$

Assuming a nonsymmetric body ($J_x \neq J_y \neq J_z$), equilibrium (or steady-state) solutions correspond to permanent rotations with constant angular velocity about each of the three axes. For the sake of discussion, let us assume that $J_x < J_y < J_z$.

Recall that in the absence of any external torques the angular momentum vector $\boldsymbol{H}$ remains constant in inertial space. Since the body rotates, $\boldsymbol{H}$ does not appear constant for an observer sitting in the body-fixed frame. Nevertheless, the magnitude of $\boldsymbol{H}$ is constant. This is evident from Eqs. (15) and (18). Thus,

$$H^2 = |\boldsymbol{H}|^2 = J_x^2\omega_x^2 + J_y^2\omega_y^2 + J_z^2\omega_z^2 \tag{32}$$

where H is a constant. In addition, conservation of energy implies that

$$T = \tfrac{1}{2}(J_x\omega_x^2 + J_y\omega_y^2 + J_z\omega_z^2) \tag{33}$$

is also constant. We can use these two expressions to determine the behavior of the angular velocity vector $\boldsymbol{\omega}$ in the body-fixed frame.

By dividing Eqs. (32) and (33) by their left-hand sides, we obtain

$$\frac{\omega_x^2}{(H/J_x)^2} + \frac{\omega_y^2}{(H/J_y)^2} + \frac{\omega_z^2}{(H/J_z)^2} = 1 \tag{34}$$

$$\frac{\omega_x^2}{(2T/J_x)} + \frac{\omega_y^2}{(2T/J_y)} + \frac{\omega_z^2}{(2T/J_z)} = 1 \tag{35}$$

These equations describe two ellipsoids in the body frame. Equation (34) is called the *angular momentum ellipsoid* and Eq. (35) is called the *kinetic energy ellipsoid*. Since the lengths of the semiaxes of these two ellipsoids differ, the ellipsoids will, in general, intersect. Their intersection defines a series of closed curves (*polhodes*), which are the paths of the the tip of the angular velocity vector as seen from the body-fixed frame. Figure 3 shows a complete set of polhodes plotted on the angular momentum ellipsoid. Equilibrium solutions correspond to the intersections of the axes with this ellipsoid. The closed curves around the permanent rotations about the x and z axes indicate that the motion is periodic and these rotations are stable. The x-shape curve in the neighborhood of the permanent rotation about the y axis (the intermediate axis of inertia) indicates that this is an unstable rotation. In fact, any small perturbation will cause the body to depart from this equilibrium point.

The previous geometric analysis shows that permanent rotations about the minor or the major principal axis of inertia are stable, whereas rotations about the axis of the intermediate moment of inertia are unstable. The reader can easily verify this behavior by throwing a book into the air about each of its principal axes and observe its subsequent motion.

Thus far, it was assumed that the kinetic energy is conserved. Often the kinetic energy is reduced steadily due to internal or external dissipative forces, for example, elasticity or drag. In this case, it can be shown that rotations about the minor axis are also unstable. The body tends to a minimum energy state which is a rotation about the major axis of inertia. In particular, for axisymmetric bodies pure spin about the symmetry axis is stable only if the symmetry axis is the major inertia axis. This was vividly demonstrated during the launch of the first U.S. satellite, Explorer I. The satellite was a prolate (pencil-shaped) axisymmetric object, designed to spin about its symmetry axis. Flexing of the four whip communication antennas, however, caused energy dissipation and decrease of the kinetic energy. The satellite ended tumbling end-to-end after just one orbit.

Despite the fact that oblate (disk-shaped) axisymmetric bodies exhibit more stable motion about their symmetry axis,

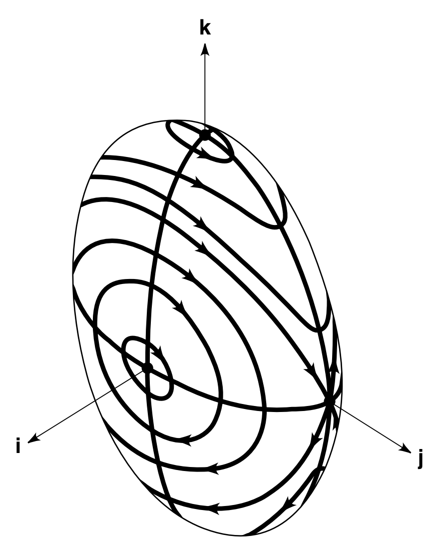

Figure 3. The closed curves on the angular momentum ellipsoid denote the path of the tip of the angular velocity vector. Rotations about the x and z axis are stable, whereas rotations about the y axis are unstable. Here y is the intermediate moment-of-inertia axis.

most often the satellites have a prolate shape. This is because the shape of the carrying rocket is prolate and elongated satellites make more efficient use of the available cargo space. Thus, stable rotations of prolate satellites about their symmetry axis require the use of some sort of stabilization.

ATTITUDE-CONTROL LAWS AND STABILIZATION

Attitude-control laws for a spacecraft can be designed based on a straightforward application of Eq. (12) or Eq. (13). In the case of passive stabilization, the control torques are generated through the interaction of the spacecraft with its environment (gravity or magnetic field, solar or aerodynamic pressure, etc.) These environmental torques are much smaller than the torques generated using active stabilization schemes. We consider here only active control methods. The external torques $\boldsymbol{M}$ acting on the spacecraft are thus almost solely due to the attitude-control system (i.e., due to gas jets firings or momentum exchange wheels). The environmental torques in this case are treated as disturbances.

For gas jets, Eq. (12) can be used directly. When momentum wheels are used as attitude control devices, the equations of motion have to be modified to take into consideration the dynamics of the wheels. For a spacecraft with three momentum wheels along the three principal axes, the equations of motion are given by

$$J\dot{\boldsymbol{\omega}} + \boldsymbol{\omega} \times J\boldsymbol{\omega} = -\boldsymbol{\omega} \times J_{\mathrm{w}}(\boldsymbol{\omega} + \boldsymbol{\nu}) - J_{\mathrm{w}}(\dot{\boldsymbol{\omega}} + \dot{\boldsymbol{\nu}}) \tag{36}$$

where $\boldsymbol{\nu}$ is the vector of the angular velocities of the three wheels relative to the spacecraft, and J_{w} is the diagonal matrix with the (polar) moments of inertia of the wheels. The control inputs are the wheel accelerations $\dot{\boldsymbol{\nu}}$. Equation (36) describes the balance between the angular momentum of the spacecraft and the wheels. It essentially states that the total angular momentum (wheels and spacecraft) remains constant.

The dynamics of the wheels are given by

$$J_{\mathrm{w}}(\dot{\boldsymbol{\omega}} + \dot{\boldsymbol{\nu}}) = -\boldsymbol{T} \tag{37}$$

where $\boldsymbol{T}$ denotes the torques developed by the electric motors of the wheels. These are internal torques, which do not affect the total angular momentum.

A preliminary feedback

$$J_{\mathrm{w}}\dot{\boldsymbol{\nu}} = -\boldsymbol{\omega} \times J_{\mathrm{w}}\boldsymbol{\nu} - \boldsymbol{M} \tag{38}$$

can be used to put the system in the standard form of Eq. (12)

$$\hat{J}\dot{\boldsymbol{\omega}} = -\boldsymbol{\omega} \times \hat{J}\boldsymbol{\omega} + \boldsymbol{M} \tag{39}$$

where $\hat{J} = J + J_{\mathrm{w}}$ is the total inertia matrix of the combined spacecraft/wheel system. Thus, regardless of whether we use gas jets or momentum wheels, Eq. (12) can be used to predict the effect of the control torques $\boldsymbol{M}$ on the body.

Typical Attitude-Control Algorithms

One typical control objective is to maintain the inertial orientation of the spacecraft fixed. This implies that the attitude control system must keep the angular velocity vector with respect to the inertial frame at zero. For small angular deviations and small angular rates, we can use the Euler angles to describe the orientation of the body frame with respect to the inertial frame. Since the angles and their rates are small, we can linearize Eqs. (13) and (24) to obtain

$$\begin{aligned} J_{\mathrm{x}}\dot{\omega}_{\mathrm{x}} &= M_{\mathrm{x}} \\ J_{\mathrm{y}}\dot{\omega}_{\mathrm{y}} &= M_{\mathrm{y}} \\ J_{\mathrm{x}}\dot{\omega}_{\mathrm{z}} &= M_{\mathrm{z}} \end{aligned} \tag{40}$$

$$\begin{aligned} \dot{\phi} &= \omega_{\mathrm{x}} \\ \dot{\theta} &= \omega_{\mathrm{y}} \\ \dot{\psi} &= \omega_{\mathrm{z}} \end{aligned} \tag{41}$$

The attitude motions about the three body axes are decoupled. The control system can independently control the motion about each individual axis. A control law of the form

$$M_{\mathrm{x}} = -k_1\phi - k_2\dot{\phi}, \quad k_1 > 0, k_2 > 0 \tag{42}$$

can be used, for example, to keep $\phi = 0$. This control law will require an attitude sensor to measure the roll angle ϕ and a rate gyro to measure $\dot{\phi}$. If no rate gyro is available a control law using *lead compensation* can be used (8)

$$\begin{aligned} M_{\mathrm{x}} &= -k(\phi - \xi) \\ \dot{\xi} &= -b\xi + (b-a)\phi \end{aligned} \tag{43}$$

where a and b positive numbers with $b > a$. The transfer function of this controller is

$$\frac{M_{\mathrm{x}}(s)}{\phi(s)} = -k\frac{s+a}{s+b} \tag{44}$$

Similar control laws can be constructed for the y (pitch) and z (yaw) axes.

The previous procedure based on linearization cannot be used when the expected deviations from the rest position are significant or when the cross-product terms in the angular velocity equation are not negligible. For large or fast angular maneuvers we need to work directly with the exact, nonlinear equations. In this case, the alternative formulation of the kinematic equations in terms of the Euler parameters in Eq. (29) becomes very useful, since we avoid the singularity of the Euler angle description. Most importantly, because of their simple structure, these equations are easier to work with than the highly nonlinear differential equations in terms of the Euler angles.

Assuming that the Euler parameters describe the *attitude error* between the current and desired orientation, we can use the control law proposed by Mortensen (9)

$$\boldsymbol{M} = -k_1\boldsymbol{\omega} - k_2\boldsymbol{q}_{\mathrm{v}}, \quad k_1 > 0, k_2 > 0 \tag{45}$$

to reorient the body to the desired attitude and keep it there. In Eq. (45), $\boldsymbol{q}_{\mathrm{v}}$ denotes the vector portion of the quaternion, $q_{\mathrm{v}} = q_1\mathbf{i} + q_2\mathbf{j} + q_3\mathbf{k}$. Note that the control law in Eq. (45) is linear, although the original equations of motion are nonlinear.

Often we wish to control only the angular velocity of the body. If the target angular velocity is zero (i.e., it is desired to bring the body to rest), the linear control law

$$\boldsymbol{M} = -k\boldsymbol{\omega}, \quad k > 0 \tag{46}$$

can be used. The difference between the control law in Eq. (45) and the control law in Eq. (46) is that in the latter the final orientation of the body is irrelevant.

To achieve an arbitrary angular velocity $\boldsymbol{\omega}_d$, the following feedback control can be used

$$\boldsymbol{M} = J\dot{\boldsymbol{\omega}}_d - kJ(\boldsymbol{\omega} - \boldsymbol{\omega}_d) + \boldsymbol{\omega} \times J\boldsymbol{\omega} \tag{47}$$

If, for instance, $\boldsymbol{\omega}_d = \omega_d \mathbf{k}$ the previous control law will generate a pure rotation of the body about its z axis with angular velocity ω_d. A special case of this situation occurs when the final spin axis of the spacecraft is also required to point along a specified direction in the inertial frame (i.e., for a spin-stabilized vehicle). The linear control given by Coppola and McClamroch (10)

$$\begin{aligned} M_x &= -(J_y - J_z)\omega_z(\dot{\theta} + \omega_d \phi) - J_x \omega_d \dot{\theta} - k_1 \dot{\phi} - k_2 \phi \\ M_y &= -(J_z - J_x)\omega_d(\dot{\phi} - \omega_d \theta) + J_y \omega_d \dot{\phi} - k_3 \dot{\theta} - k_4 \theta \\ M_z &= -k_5(\omega_z - \omega_d) \end{aligned} \tag{48}$$

for some positive scalars k_i, will keep the body z axis aligned with the inertial Z axis (assuming that ω_x, ω_y, ϕ, θ are small), whereas the control law

$$\begin{aligned} M_x &= -k_1\left(\frac{\sin\phi\cos\theta}{1+\cos\phi\cos\theta}\right) - k_2\omega_x \\ M_y &= -k_1\left(\frac{\sin\theta}{1+\cos\phi\cos\theta}\right) - k_3\omega_y \\ M_z &= -k_3(\omega_z - \omega_d) \end{aligned} \tag{49}$$

for some positive k_i, can be used to bring the spin-axis (assumed to be the body z axis) along the inertial Z axis from almost every (not necessarily small) initial state (11).

Spacecraft in Orbit. Another important special case of the previous control laws is the stabilization of a spacecraft in a circular orbit of radius R_c, such that its z axis points always towards the Earth. The orbital angular velocity is

$$\Omega = \sqrt{\frac{g}{R_c}} \tag{50}$$

In this case it is convenient to choose an inertial frame that is parallel to a local-vertical, local-horizontal frame attached at the center of mass of the spacecraft. The X axis of this frame points along the direction of the orbital velocity (local horizontal), the Z axis points along the center of the Earth (local vertical), and Y points along the negative of the angular velocity vector $\boldsymbol{\Omega}$ of the orbit. Describing the orientation of the spacecraft with respect to this frame, the equations of motion can be written as (8,10)

$$\begin{aligned} J_x\dot{\omega}_x &= -\Omega(J_y - J_z)\omega_z - 3\Omega^2(J_y - J_z)\phi + M_x \\ J_y\dot{\omega}_y &= 3\Omega^2(J_x - J_z)\theta + M_y \\ J_z\dot{\omega}_z &= \Omega(J_y - J_x)\omega_x + M_z \end{aligned} \tag{51}$$

$$\begin{aligned} \dot{\phi} &= \Omega\psi + \omega_x \\ \dot{\theta} &= \Omega + \omega_y \\ \dot{\psi} &= -\Omega\phi + \omega_z \end{aligned} \tag{52}$$

These equations reveal that the pitching motion is decoupled from roll/yaw motions. The control law

$$\begin{aligned} M_x &= -4\Omega^2(J_z - J_y)\phi - k_1\phi - k_2\dot{\phi} - \Omega(J_x + J_z - J_y)\dot{\psi} \\ M_y &= -3\Omega^2(J_x - J_z)\theta - k_3\theta - k_4\dot{\theta} \\ M_z &= \Omega^2(J_y - J_x)\psi - k_5\psi - k_6\dot{\psi} + \Omega(J_x + J_z - J_y)\dot{\phi} \end{aligned} \tag{53}$$

for some positive numbers k_i, can be used to make the spacecraft rotate about its y axis such that its z axis points always toward the Earth.

Optimal Reorientation Maneuvers. Because of limited onboard resources (e.g., power consumption or propellant), a spacecraft control system may be required to achieve the control objectives in the presence of certain constraints. For instance, it is clearly desirable to design control algorithms that minimize the fuel consumption during a particular maneuver (assuming gas jets are used as attitude actuators). Another example is the reorientation of an optical telescope or antenna in minimum time.

For small-angle reorientation maneuvers about individual principal axes, the linear equations in Eqs. (40) and (41) can be used. Linear quadratic methods provide optimal controls for a quadratic penalty on the error and the control input. These methods have been discussed elsewhere (12,13).

Referring to Eq. (13), Windeknecht (14) showed that the control law that minimizes the quantity

$$\mathscr{J} = |\boldsymbol{H}(t_f)| + \lambda \int_0^{t_f} |\boldsymbol{M}(t)|^2\, dt \tag{54}$$

is given by

$$\boldsymbol{M}^* = -\frac{\boldsymbol{H}}{(t_f - t) + \lambda} \tag{55}$$

Kumar (15) showed that the optimal control minimizing the quantity

$$\mathscr{J} = \int_0^{t_f} |\boldsymbol{H}|^2\, dt + \lambda \int_0^{t_f} |\boldsymbol{M}|^2\, dt \tag{56}$$

is given by

$$\boldsymbol{M}^* = -\gamma(t)\boldsymbol{H} \tag{57}$$

where

$$\gamma(t) = \frac{1}{\sqrt{\lambda}} \tanh\left(\frac{t_f - t}{\sqrt{\lambda}}\right) \tag{58}$$

For $t_f \to \infty$ the previous expression reduces to the linear control

$$\boldsymbol{M}^* = -\frac{\boldsymbol{H}}{\sqrt{\lambda}} \tag{59}$$

The previous control laws minimize the *energy* required to perform the maneuver. Often it is more relevant to minimize the fuel expenditure.

Fuel consumption is proportional to the magnitude of the control torque $|\boldsymbol{M}|$. The *minimum-fuel* control law which takes the system to the rest position is thus derived by minimizing

$$\mathscr{J} = \int_0^{t_f} |\boldsymbol{M}|\, dt \tag{60}$$

where the final time t_f is not prescribed. The optimal feedback control law is given by

$$\boldsymbol{M}^* = -\bar{M}\frac{\boldsymbol{H}}{|\boldsymbol{H}|} \tag{61}$$

where $\bar{M}$ is a constraint on the available control magnitude, $|\boldsymbol{M}| \le \bar{M}$ (16).

The control law in Eq. (61) is also the *minimum-time* control law for the system in Eq. (13). This control law does not deal with the final orientation of the spacecraft, however. Minimum-time reorientation maneuvers where the final attitude is also of interest have been treated extensively in the literature (17,18). Analytic solutions are extremely difficult to find in this case. For large-angle (slew) maneuvers, in particular, one almost always needs to resort to numerical methods using Pontryagin's Maximum Principle (17,19). Nevertheless, a minimum-time three-dimensional maneuver is not a minimum-time rotation about the corresponding eigenaxis (20).

Explicit calculation of the minimum-time control law is possible if we assume that the angular displacements are small. In this case the linearized equations in Eqs. (40) and (41) can be used, and the optimal control is *bang–bang control* (i.e, one that switches between the maximum and minimum

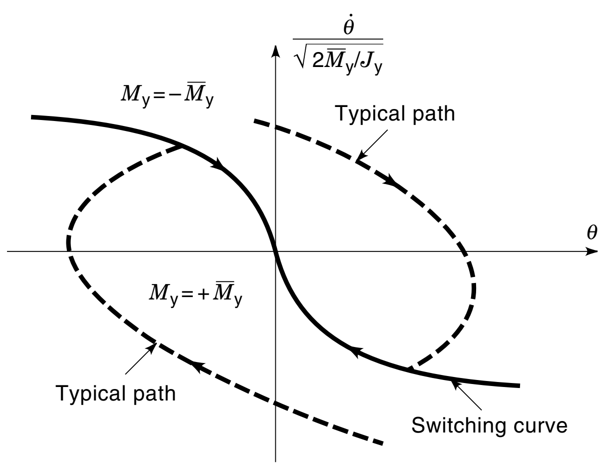

Figure 4. Bang–bang minimum time control of a single-axis attitude maneuver. If the initial orientation and velocity of the body is below the switching curve, the control logic will switch from the maximum to the minimum possible torque. The opposite is true if the initial condition is above the switching curve.

value of the torque). For instance, assuming that the maximum available torque about the pitch axis is $\bar{M}_y$, the control law that will bring the motion about the y body axis to rest in minimum time switches from $-\bar{M}_y$ to $+\bar{M}_y$ (or vice versa) according to whether the initial state $(\theta,\dot{\theta})$ is above or below the *switching curve* in Fig. 4. The switching occurs when θ and $\dot{\theta}$ satisfy the *switching condition*

$$\dot{\theta}^2 = \pm\theta\left(\frac{2\bar{M}_y}{J_y}\right) \tag{62}$$

which is the equation that defines the switching curve. A summary of the minimum-time attitude maneuver literature can be found in the survey article by Scrivener and Thomson (21).

AIRCRAFT ATTITUDE CONTROL

Although similar, attitude-control problems for aircraft are much more challenging than attitude-control problems for spacecraft. The main difference between an aircraft and a spacecraft is the fact that the former flies in the atmosphere. The principal forces and moments acting on an aircraft are generated by the interaction of the airplane with the air flow. These forces are the same ones used for attitude control. Moreover, since the same forces also affect the aircraft's center of mass, the translational and rotational equations are coupled.

The aerodynamic forces acting on an aircraft in the atmosphere are proportional to the air density and the square of the airspeed (the relative velocity of the airplane to the air flow). The main aerodynamic forces acting on an aircraft are the *drag,* which is opposite to the direction of the airplane's velocity vector, and the *lift,* which is perpendicular to the velocity vector. Lift opposes gravity and is the force that makes airplanes stay aloft. Drag opposes the motion of the airplane through the air and is responsible for most of the fuel consumption. Other significant forces acting on an airplane are the force of gravity and the thrust from the engines.

Aircraft Dynamics

As for spacecraft problems, the orientation of an airplane is determined by the relative angular displacements between a reference frame fixed in the airplane and an inertial frame. For most problems in airplane dynamics an axis system fixed to the Earth can be used as an inertial reference frame. There are several choices for the body reference frame. The body axes are aligned such that the x axis is along the longitudinal fuselage axis, the y axis is along the right wing, and the z axis is mutually perpendicular to the x and y axes. The wind axes are defined such that the x axis is along the direction of the relative wind. The angles α and β, defined by performing a rotation about the body y axis, followed by a rotation about the new z axis, until the body x axis is along the velocity vector, are called the *angle of attack* and *sideslip angle,* respectively. A positive angle of attack corresponds to a negative rotation about the y axis. The sideslip angle is positive if the rotation about the z axis is positive. The wind axis is the natural choice for analyzing the aerodynamic forces and moments. The stability axes are defined by the angle α between the body x axis and the stability x axis. Although all the previous sets of axes are referred to in the literature as body axes, only the first one is body-fixed. The orientation of the stability and wind axes may vary with flight conditions, but in most cases α and β are small, so the stability and wind axes are close to the body-fixed axes.

The transformation from body to stability axes is given by

$$\begin{bmatrix} x \\ y \\ z \end{bmatrix}_S = \begin{bmatrix} \cos\alpha & 0 & \sin\alpha \\ 0 & 1 & 0 \\ -\sin\alpha & 0 & \cos\alpha \end{bmatrix} \begin{bmatrix} x \\ y \\ z \end{bmatrix}_B \tag{63}$$

whereas the rotation from stability to wind axes is given by

$$\begin{bmatrix} x \\ y \\ z \end{bmatrix}_W = \begin{bmatrix} \cos\beta & \sin\beta & 0 \\ -\sin\beta & \cos\beta & 0 \\ 0 & 0 & 1 \end{bmatrix} \begin{bmatrix} x \\ y \\ z \end{bmatrix}_S \tag{64}$$

Subsequently, the rotation matrix from body to wind axes is given by

$$\begin{bmatrix} \cos\alpha\cos\beta & \sin\beta & \sin\alpha\cos\beta \\ -\cos\alpha\sin\beta & \cos\beta & -\sin\alpha\sin\beta \\ -\sin\alpha & 0 & \cos\alpha \end{bmatrix} = \begin{bmatrix} \cos\beta & \sin\beta & 0 \\ -\sin\beta & \cos\beta & 0 \\ 0 & 0 & 1 \end{bmatrix} \begin{bmatrix} \cos\alpha & 0 & \sin\alpha \\ 0 & 1 & 0 \\ -\sin\alpha & 0 & \cos\alpha \end{bmatrix} \tag{65}$$

The body, wind, and stability axes for positive α and β are shown in Fig. 5. From Fig. 5 we have immediately that the angle of attack and the sideslip angle satisfy the following expressions

$$\tan\alpha = \frac{w}{u}, \quad \sin\beta = \frac{v}{V_T} \tag{66}$$

where u, v, and w are the components of the relative airspeed velocity of the airplane in the body axes. The magnitude $V_T = (u^2 + v^2 + w^2)^{1/2}$ of the relative velocity is called the *true airspeed.* If the xy plane is a plane of symmetry of the airplane

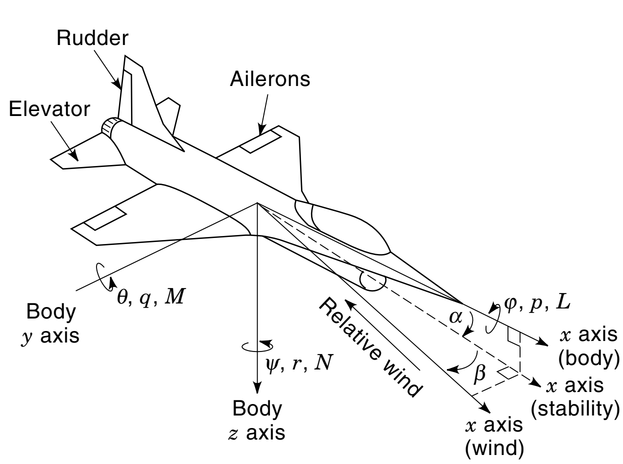

Figure 5. Body reference frames on an airplane. The stability axes differ from the wind axes by the sideslip angle β, and the body-fixed axes differ from the stability axes by the angle of attack α. The angles α and β change as the relative velocity of the airplane to the wind changes.

(as is often the case), the off-diagonal terms in the inertia matrix J_{xy} and J_{yz} are zero. Following the standard notation in aircraft literature (22,23), we denote the three components of the angular velocity vector in body axes by p, q, and r, respectively and the components of the applied torque by L, M, and N.

The equations of motion in Eq. (12) are then written as

$$\begin{aligned} L &= J_x\dot{p} - J_{xz}\dot{r} + qr(J_z - J_y) - J_{xz}pq \\ M &= J_y\dot{q} + rp(J_x - J_z) - J_{xz}(p^2 - r^2) \\ N &= -J_{xz}\dot{p} + J_z\dot{r} + pq(J_y - J_x) + J_{xz}qr \end{aligned} \tag{67}$$

The moments L, M, and N represent the roll, pitching, and yawing moments, respectively. They are defined in terms of dimensionless aerodynamic coefficients C_l, C_m, and C_n as follows

$$\begin{aligned} L &= \bar{q}SbC_l \\ M &= \bar{q}ScC_m \\ N &= \bar{q}SbC_n \end{aligned} \tag{68}$$

where $\bar{q}$ is the free-stream dynamic pressure, defined by

$$\bar{q} = \frac{1}{2}\rho V_T^2 \tag{69}$$

S is the airplane wing reference area, b is the wing span, and c is the wing mean geometric chord. In Eq. (69), ρ is the air density (1.225 kg/m^3 at the sea level).

The dimensionless coefficients C_l, C_m, and C_n measure the effectiveness of the airplane's aerodynamic surfaces in producing moments and depend on several factors, such as the aerodynamic angles α and β, control surface deflections, engine power level, airplane geometry, and configuration. For small deviations of these parameters, the moments L, M, and N can be approximated by the expansions given in Pachter and Houpis (24)

$$\begin{aligned} L &= \bar{q}Sb\left(\frac{b}{2V_T}C_{l_p}p + \frac{b}{2V_T}C_{l_r}r + C_{l_\beta}\beta + C_{l_{\delta_a}}\delta_a + C_{l_{\delta_r}}\delta_r\right) \\ M &= \bar{q}Sc\left(C_{m_0} + C_{m_\alpha}\alpha + \frac{c}{2V_T}C_{m_q}q + \frac{c}{2V_T}C_{m_{\dot\alpha}}\dot\alpha + C_{m_{\delta_e}}\delta_e\right) \\ N &= \bar{q}Sb\left(\frac{b}{2V_T}C_{n_p}p + \frac{p}{2V_T}C_{n_r}r + C_{n_\beta}\beta + C_{n_{\delta_a}}\delta_a + C_{n_{\delta_r}}\delta_r\right) \end{aligned} \tag{70}$$

where δ_e denotes the deflection angle for the elevator, δ_r the angle for the rudder, and δ_a for the ailerons. The coefficients C_{l_p}, C_{n_β}, $C_{m_{\dot\alpha}}$, . . ., are called the *stability derivatives.* The stability of an airplane about an equilibrium configuration depends upon these coefficients.

As shown by McLean (25), for large aircraft, such as civilian passenger airplanes and transports, which cannot generate large angular velocities, Eq. (67) can be approximated by

$$\begin{aligned} L &= J_x\dot{p} - J_{xz}(\dot{r} + pq) \\ M &= J_y\dot{q} + J_{xz}(p^2 - r^2) \\ N &= J_z\dot{r} - J_{xz}(\dot{p} - qr) \end{aligned} \tag{71}$$

Equation (67) can be inverted to obtain

$$\dot{p} = \frac{J_{xz}}{\Delta}(J_x - J_y + J_z)pq - \frac{J_z^2 - J_z J_y + J_{xz}^2}{\Delta}qr + \frac{J_z}{\Delta}L + \frac{J_{xz}}{\Delta}N$$
$$\dot{q} = \frac{J_z - J_x}{J_y}pr - \frac{J_{xz}}{J_y}(p^2 - r^2) + \frac{1}{J_y}M$$
$$\dot{r} = \frac{J_x^2 - J_y J_x + J_{xz}^2}{\Delta}pq - \frac{J_{xz}}{\Delta}(J_x - J_y + J_z)qr + \frac{J_{xz}}{\Delta}L + \frac{J_x}{\Delta}N \quad (72)$$

where $\Delta = J_x J_z - J_{xz}^2$. Once the moments L, M, and N are known, the angular velocity can be computed by integrating Eq. (72).

Euler Angles

The orientation of an airplane is given by the three Euler angles ϕ, θ, and ψ from Eq. (22), also referred to as *roll, pitch,* and *yaw,* respectively. The kinematic equations of the airplane's rotational motion are thus given by Eq. (24), repeated below for convenience

$$\begin{aligned} \dot{\phi} &= p + q\sin\phi\tan\theta + r\cos\phi\tan\theta \\ \dot{\theta} &= q\cos\phi - r\sin\phi \\ \dot{\psi} &= (q\sin\phi + r\cos\phi)\sec\theta \end{aligned} \quad (73)$$

Equations (72) and (73) can be integrated to completely describe the attitude evolution of the aircraft. It should be pointed out, however, that the aerodynamic forces and moments depend on the altitude and speed of the airplane. The rotational equations are thus coupled with the translational (flight path) equations of motion. A complete, six-degree-of-freedom system that includes the translational equations is required to accurately describe the current position and velocity of the airplane. The complete nonlinear equations can be decomposed into the longitudinal equations, which describe the motion in the *xz* plane, and the lateral equations, which describe the motion outside the *xz* plane. The longitudinal part of the airplane's motion includes, in addition to θ and q, the forward and vertical velocity of the center of mass. The lateral equations, in addition to ϕ, ψ, p, and r will include the side velocity of the center of mass. A more complete discussion of the airplane's complete set of equations of motion may be consulted (see, for example, Ref. 26).

Aircraft Actuators

Control of an airplane is achieved by providing an incremental lift force on one or more of the airplane's surfaces. Because these control surfaces are located at a distance from the center of mass, the incremental lift force generates a moment about the airplane's center of mass. The magnitude of the moment is proportional to the force and the distance of the control surface from the center of the mass.

The main control actuators used for changing an airplane's attitude motion are the elevators, the rudder, and the ailerons. Additional configurations may include canards (small surfaces located ahead of the main wing) or thrust vectoring devices (for military aircraft). Figure 5 shows the main control surfaces of an airplane.

Elevators. Elevators are relatively small surfaces located close to the tail of the airplane. Deflecting the elevators produces moments about the pitch axis of the airplane. Elevators are thus, primarily, pitch-control devices. The transfer function between the elevator deflection δ_e and the pitch angle θ is given by

$$\frac{\theta(s)}{\delta_e(s)} = \frac{K_\theta(s^2 + 2\zeta_\theta\omega_\theta s + \omega_\theta^2)}{(s^2 + 2\zeta_{ph}\omega_{ph}s + \omega_{ph}^2)(s^2 + 2\zeta_{sp}\omega_{sp}s + \omega_{sp}^2)} \quad (74)$$

The ζ_{ph}, ω_{ph} and ζ_{sp}, ω_{sp} are the damping ratio and natural frequency of the *phugoid* and *short-period modes,* respectively.

Rudders. The rudder is a hinged flap that is part of the vertical surface located at the tail of the airplane. It is primarily a yaw-control device and is the main directional control device of the airplane. In addition to directional control, the rudder is used to compensate for unwanted directional yaw deflections caused by the airelons when an airplane is banked to execute a turning maneuver.

Airelons. Airelons differ from the previous two control devices, because they incorporate two lifting surfaces. Ailerons are located at the tips of the main wings of the airplane. Roll control is achieved by the differential deflection of the ailerons. They modify the lift distribution of the wings (increase it in one wing and decrease it in the other) so that a moment is created about the x axis.

Spoilers. Roll moment is also produced by deflecting a wing spoiler. Wing spoilers are small surfaces located on the upper wing surface and cause flow separation when deflected. Flow separation in turn causes a reduction in lift. If only one spoiler is used at a time, the lift differential between the two wings will cause a rolling moment. In some aircraft roll control is also produced by tail surfaces moving differentially.

Roll. The rolling (lateral) motion is not, in general, decoupled from the yawing (directional) motion. The transfer functions from δ_a and δ_r to ϕ and ψ are coupled. The transfer function from aileron deflection to roll angle ϕ is given by

$$\frac{\phi(s)}{\delta_a(s)} = \frac{K_\phi(s^2 + 2\zeta_\phi\omega_\phi s + \omega_\phi^2)}{(s + 1/T_s)(s + 1/T_r)(s^2 + 2\zeta_D\omega_D s + \omega_D^2)} \quad (75)$$

whereas the transfer function from rudder deflection to yaw angle ψ is given by

$$\frac{\psi(s)}{\delta_r(s)} = \frac{K_\psi(s^2 + 2\zeta_\psi\omega_\psi s + \omega_\psi^2)}{(s + 1/T_s)(s + 1/T_r)(s^2 + 2\zeta_D\omega_D s + \omega_D^2)} \quad (76)$$

Similar expressions hold for the transfer functions $\phi(s)/\delta_r(s)$ and $\psi(s)/\delta_a(s)$. These equations should be used with caution since, as mentioned earlier, the lateral/directional motion is inherently a multi-input/multi-output system.

The quadratic term in the denominator in Eqs. (75) and (76) corresponds to the *dutch roll mode.* The first term in the denominator corresponds to the *spiral mode* and the second term to the *rolling subsidence mode.* For most aircraft T_s is much larger than T_r and the quadratic terms in the numerator and denominator in Eq. (75) are quite close. Equation (75) can therefore be approximated by

$$\frac{\phi(s)}{\delta_a(s)} = \frac{K_\phi}{s(s + 1/T_r)} \quad (77)$$

The transfer function from δ_r to ψ is more difficult to approximate. Often, the dutch roll approximation found in McLean (25)

$$\frac{\psi(s)}{\delta_r(s)} = \frac{K_\psi}{(s^2 + 2\zeta_D\omega_D s + \omega_D^2)} \tag{78}$$

is good enough.

The short period, the roll, and the dutch-roll modes are the main principal modes associated with the rotational motion of the aircraft and are much faster than the phugoid and spiral modes, which are primarily associated with changes of the flight-path (translational motion). The slow phugoid and spiral modes can be controlled adequately by the pilot. Control systems are required, in general, for controlling or modifying the rotational modes. In addition, the maneuverability of the aircraft is primarily determined by the rotational modes.

Stability Augmentation and Aircraft Attitude-Control Systems

An *automatic flight control system* (AFCS) typically performs three main tasks: (1) modifies any unsatisfactory behavior of the aircraft's natural flying characteristics, (2) provides relief from the pilot's workload during normal cruising conditions or maneuvering, and (3) performs several specific functions, such as automatic landing. In addition, an AFCS may perform several secondary operations, such as engine and aircraft component monitoring, flight-path generation, terrain-following, collision avoidance. Here we briefly outline the fundamental operations of only the first two tasks.

Control systems that are used to increase the damping or stiffness of the aircraft motion so as to provide artificial stability for an airplane with undesirable flying characteristics are called *stability augmentation systems* (SAS). Typical uses of SAS are in increasing the damping ratio of the short period motion in pitch (pitch rate SAS), providing damping in the roll subsidence mode (roll rate SAS), modifying the dutch roll mode (yaw rate SAS), and increasing the maneuverability of the aircraft by reducing static stability margins (relaxed static stability SAS).

The SAS typically uses gyroscopes as sensors to measure the body-axes angular rates, processes them on-board using a flight-control computer, and generates the appropriate signals to the servomechanisms that drive the aerodynamic control surfaces.

In addition to stability augmentation systems, which are used to modify the characteristics of the natural modes of the airplane, *attitude-control systems* (ACS) are used to perform more complex tasks. In contrast to the SAS, they use signals from many sensors and control several of the aircraft's surfaces simultaneously. As a result, attitude control systems are multivariable control systems and therefore more complex in their operation than SAS. Common ACS for a typical aircraft are pitch ACS, roll angle ACS, coordinated-turn control systems, wing levellers, and sideslip suppression systems. A more in-depth discussion of ACS can be found in McLean (25) and Stevens and Lewis (23).

The aircraft dynamics change considerably with the flight conditions, such as speed and altitude. The control design process involves linearization of the nonlinear equations of motion about steady state (trim) conditions. Steady-state aircraft flight is defined as a condition where all motion (state) variables are constant or zero. That is, linear and angular velocity are constant (or zero) and all accelerations are zero. Examples of steady-state flight conditions involving the rotational degrees of freedom include: (1) steady turning flight ($\dot{\psi} = \dot{\theta} = 0$), (2) steady pull-up ($\phi = \dot{\phi} = \dot{\psi} = 0$), and (3) steady roll ($\dot{\theta} = \dot{\psi} = 0$).

A control system designed for a certain steady-state condition may perform very poorly at another condition or even lead to instability. A control system must therefore be adapted during the flight to accommodate the wide variations in aircraft dynamics occurring over the flight envelope. Typically, several controllers are designed for different conditions and then *gain-scheduled* during the flight. Gain scheduling amounts to switching between the different controllers or adjusting their parameters (i.e., gains) as the airplane's flight conditions change. Dynamic pressure is commonly used to schedule the controllers because it captures changes of both altitude and speed. Other parameters, such as angle of attack are used as well. Care must be taken when switching controllers during gain scheduling to avoid unacceptable transients. Extensive simulations are required to ensure that the gain-scheduled control system performs satisfactorily. The U.S. government periodically releases a series of publications (e.g., 27), with guidelines and specifications for acceptable performance of flight-control systems.

ATTITUDE CONTROL IN ROBOTICS

One of the main problems in robotics is the derivation of algorithms to actively control the position and orientation of the end-effector of a robotic manipulator, whether it is a video camera, a gripper, or a tool. The position and orientation of the end-effector is completely determined by the position and linear or angular displacements of the robot joints. For the sake of discussion, we henceforth consider a robot consisting of revolute joints only. The case with prismatic joints can be treated similarly. For a robot manipulator made of n links interconnected by revolute joints, the joint variables $\beta_1, \ldots, \beta_n$ are the relative angles between the links. The orientation and velocity of the end effector is then completely determined by the angles β_i and their rates $\dot{\beta}_i$ ($i = 1, \ldots, n$).

To describe the orientation of the end effector with respect to the inertial space, we choose a reference frame fixed at the end effector. We call this frame the *end-effector frame* or the *task frame* (28). The *inertial frame* (also called the *base* or *world frame*) is usually established at the base of the robot. The end-effector orientation is then given by the rotation matrix R between these two reference frames. Relative rotation of the robot joints induces an angular velocity of the task frame with respect to the base frame.

Three Euler angles ϕ, θ, and ψ (roll, pitch, and yaw) can be used to parameterize the rotation matrix R between the two frames. These angles are the same as the ones in Figure 2. For a gripper, the roll angle ϕ describes relative rotation about an axis extending forward from the manipulator (the roll axis). The pitch angle θ describes relative rotation about the axis parallel to the axis connecting the gripper's fingers (pitch axis) and perpendicular to the roll axis. Finally, the yaw angle ψ describes a rotation about an axis perpendicular to both the roll and the pitch axis. As discussed elsewhere (28), the x, y, and z directions of the tool frame are labeled frequently as a, s, and n, respectively. The terminology arises from the fact that the direction a (or x) is the *approach* direction (i.e., this is the direction that the gripper typically approaches an object). The s (or y) direction is the *sliding* direction (i.e., the direction along which the fingers of the gripper slide to close or open). The n (or z) direction is normal to the plane defined by the a and s directions. The (a, s, n) frame attached to a gripper is shown in Figure 6.

The roll, pitch, and yaw angles completely describe the orientation of the end effector. They are given by

$$\begin{aligned} \phi &= f_1(\beta_1, \ldots, \beta_n) \\ \theta &= f_2(\beta_1, \ldots, \beta_n) \\ \psi &= f_3(\beta_1, \ldots, \beta_n) \end{aligned} \tag{79}$$

where the functions f_1, f_2, and f_3 are determined by the specific geometry of the manipulator. Differentiating the previous equation with respect to time, one obtains

$$\begin{aligned} \dot{\phi} &= \frac{\partial f_1}{\partial \beta_1}\dot{\beta}_1 + \cdots + \frac{\partial f_1}{\partial \beta_n}\dot{\beta}_n \\ \dot{\theta} &= \frac{\partial f_2}{\partial \beta_1}\dot{\beta}_1 + \cdots + \frac{\partial f_2}{\partial \beta_n}\dot{\beta}_n \\ \dot{\psi} &= \frac{\partial f_3}{\partial \beta_1}\dot{\beta}_1 + \cdots + \frac{\partial f_3}{\partial \beta_n}\dot{\beta} \end{aligned} \tag{80}$$

We can use Eqs. (24) and (80) to obtain a relation between the angular velocity vector $\boldsymbol{\omega}$ expressed in the end-effector frame as a function of the rates of change of the joint angles β_i as follows

$$\omega = J(\beta)\dot{\beta} \tag{81}$$

where $J(\beta)$ is a $3 \times n$ matrix and $\beta = (\beta_1, \ldots, \beta_n)$. The matrix $J(\beta)$ is often called the *Jacobian kinematics*.

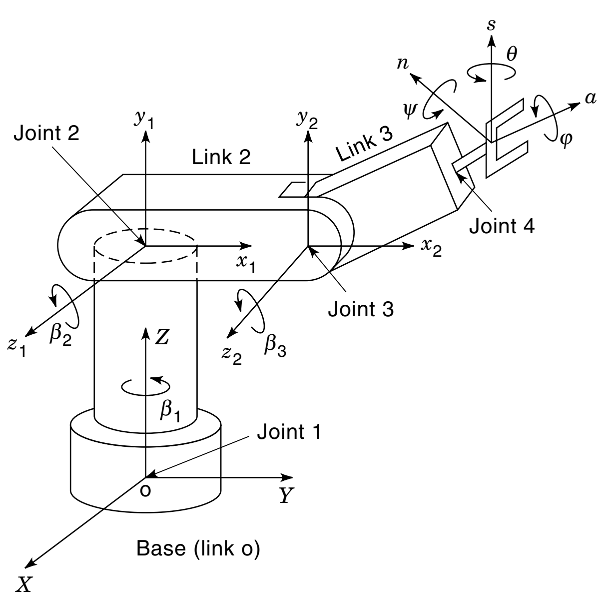

Figure 6. Typical robotic manipulator consisting only of revolute joints. The attitude of the gripper is given by the orientation of the (a, s, n) body frame. The geometry of the manipulator determines the orientation of this frame with respect the the joint angles β_1, β_2, and β_3.

The torques generated at the joints will specify a commanded time history for $\beta_i(t)$ and $\dot{\beta}_i(t)$. Equations (79) and (81) can be used to find the corresponding angular position and velocity of the end effector. This is the so-called *forward kinematics* problem.

As an example, consider the general equation of a robotic manipulator (29)

$$M(\beta)\ddot{\beta} + C(\beta, \dot{\beta})\dot{\beta} + K(\beta) = \tau \tag{82}$$

These equations are derived using the classical Lagrange equations (e.g., 6). The matrix $M(\beta)$ is the mass matrix, the term $C(\beta,\dot{\beta})\,\dot{\beta}$ contains the Coriolis acceleration terms, and $K(\beta)$ contains all conservative forces (e.g., gravity). A control law for a robotic manipulator will generate the torques τ at the robot joints. Assuming an actuator (i.e., motor) at each joint, a control law can be devised to track some prespecified trajectory $\beta_d(t)$ in terms of the joint angles β_i. For example, the control law

$$\tau = M(\beta)v + C(\beta, \dot{\beta})\dot{\beta} + K(\beta) \tag{83}$$

where

$$v = \ddot{\beta}_d - 2\lambda(\dot{\beta} - \dot{\beta}_d) - \lambda^2(\beta - \beta_d), \quad \lambda > 0 \tag{84}$$

will force $\beta(t) \to \beta_d(t)$ as $t \to \infty$.

Very often, the inverse problem is of interest. For example, the desired orientation and angular velocity of the end effector may be known or specified by the robot's mission requirements. In those cases, it may be necessary to find the required velocities and positions at the joints, given the angular orientation and velocity of the end effector. The problem of finding the joint variables for a given position and orientation of the end effector is called the *inverse kinematics* problem, and it is much more difficult than the forward kinematics problem. The solution of the inverse problem is obtained by inverting Eqs. (79) and (81) for given ω and (ϕ, θ, ψ). In general, because $n \geq 3$, this problem has more than one solution. The best solution $(\beta, \dot{\beta})$ depends on the specific application. The minimum-norm (least-squares) solution of Eq. (81) is given by

$$\dot{\beta} = J^{\dagger}(\beta)\eta \tag{85}$$

where $J^{\dagger}(\beta) = J^T(\beta)\,[J(\beta)J^T(\beta)]^{-1}$ denotes the Moore-Penrose pseudoinverse of the matrix $J(\beta)$ and where η denotes the vector of the Euler angles and the angular velocity. Equation (85) provides the minimum joint velocity $\dot{\beta}$, which gives the desired end-effector velocity ω.

CURRENT TRENDS

Several methodologies exist for stabilizing or controlling a rigid spacecraft when at least three independent control inputs are available. Some of these methodologies have been presented earlier. More challenging is the case when one or more actuators (either gas jets or momentum wheels) have failed. The theoretical investigation of this problem was initially addressed by Crouch (30). Several control laws were subsequently proposed, both for the angular-velocity equations (e.g., 31), and the complete velocity/orientation equations (e.g., 32,33).

Controlling flexible spacecraft also presents great challenges. Control laws using on–off thrusters, for example, may excite the flexible modes of lightweight space structures, such as trusses or antennas. Modern control theory based on state-space models has been used to control these systems with great success. An in-depth discussion on the effect of flexibility on spacecraft reorientation maneuvers can be found in the literature (12,34,35).

Research into fail-safe control systems for aircraft has also been an active area. The main emphasis has been placed on the design of reconfigurable flight-control systems and, more specifically, attitude-control systems. The idea is to construct intelligent control systems with high levels of autonomy that can reprogram themselves in case of an unexpected failure, so as to fly and land the airplane safely. The use of multivariable modern control theory (23) along with the use of redundant sensors and actuators and smart materials promise to change the current method of designing and implementing control systems for aircraft.

Traditionally, the airplane control surfaces are connected directly to the cockpit through mechanical and hydraulic connections. A pilot command corresponds to a proportional surface deflection. In many recent military and civilian aircraft, the commands from the pilot are sent electronically to the control computer instead. The computer generates the appropriate control deflection signals based on its preprogrammed control law. This method is called *fly-by-wire,* since the pilot does not have direct command of the control surfaces. The on-board control computer is responsible for interpreting and executing the pilot commands. Redundant computers or backup mechanical connections are used to guard against possible computer failures. The term *fly-by-light* is also used when the pilot and control commands are sent using fiber-optic connections.

BIBLIOGRAPHY

1. J. R. Wertz, *Spacecraft Attitude Determination and Control,* Dordrecht: D. Reidel, 1980
2. W. Wiesel, *Spaceflight Dynamics,* New York: McGraw-Hill, 1989.
3. T. R. Kane, P. W. Likins, and P. A. Levinson, *Spacecraft Dynamics,* New York: McGraw-Hill, 1983.
4. M. D. Shuster, A survey of attitude representations, *J. Astronaut. Sci.* **41** (4): 439–517, 1993.
5. J. Stuelpnagel, On the parameterization of the three-dimensional rotation group, *SIAM Rev.* **6** (4): 422–430, 1964.
6. D. T. Greenwood, *Principles of Dynamics,* Englewood Cliffs, NJ: Prentice-Hall, 1988.
7. E. T. Whittaker, *Analytical Dynamics of Particles and Rigid Bodies,* New York: Dover, 1944.
8. A. E. Bryson, *Control of Spacecraft and Aircraft,* Princeton, NJ: Princeton University Press, 1994.
9. R. E. Mortensen, A globally stable linear attitude regulator, *Int. J. Cont.* **8** (3): 297–302, 1968.
10. V. Coppola and H. N. McClamroch, Spacecraft attitude control, in W. S. Levine (ed.), *The Control Handbook,* Boca Raton, FL: CRC Press, 1996.
11. P. Tsiotras and J. M. Longuski, Spin-axis stabilization of symmetric spacecraft with two control torques, *Syst. Cont. Lett.* **23** (6): 395–402, 1994.
12. J. L. Junkins and J. Turner, *Optimal Spacecraft Rotational Maneuvers,* New York: Elsevier, 1986.
13. A. E. Bryson and Y.-C. Ho, *Applied Optimal Control: Optimization, Estimation, and Control,* Washington, DC: Hemisphere, 1975.
14. T. G. Windeknecht, Optimal stabilization of rigid body attitude, *J. Math. Anal. Appl.* **6** (2): 325–335, 1963.
15. K. S. P. Kumar, On the optimum stabilization of a satellite, *IEEE Trans. Aerospace Electron Syst.,* **1** (2): 82–83, 1965.
16. M. Athans, P. L. Falb, and R. T. Lacoss, Time-, fuel-, and energy-optimal control of nonlinear norm-invariant systems, *IRE Trans. Automatic Contr.,* **8**: 196–202, 1963.
17. J. L. Junkins, C. K. Carrington, and C. E. Williams, Time-optimal magnetic attitude maneuvers, *J. Guid., Contr., Dynam.,* **4** (4): 363–368, 1981.
18. J. R. Etter, A solution of the time-optimal Euler rotation problem, in *Proceedings of the AIAA Guidance, Navigation, and Control Conference,* Vol. 2, Washington, DC: AIAA, 1989, pp. 1441–1449.
19. E. B. Lee and L. Markus, *Foundations of Optimal Control Theory.* Malabar, FL: Krieger, 1986.
20. K. D. Bilimoria and B. Wie, Time-optimal reorientation of a rigid axisymmetric spacecraft, in *Proceedings of the AIAA Guidance, Navigation, and Control Conference,* Washington, DC: AIAA, 1991, Paper 91-2644-CP.
21. S. L. Scrivener and R. C. Thomson, Survey of time-optimal attitude maneuvers, *J. Guid., Contr., Dynam.,* **17** (2): 225–233, 1994.
22. C. R. Nelson, *Flight Stability and Automatic Control,* New York: McGraw-Hill, 1989.
23. B. L. Stevens and F. L. Lewis, *Aircraft Control and Simulation,* New York: Wiley, 1992.
24. M. Pachter and C. H. Houpis, Flight control of piloted aircraft, in W. S. Levine (ed), *The Control Handbook,* Boca Raton, FL: CRC Press, 1996.
25. D. McLean, *Automatic Flight Control Systems,* New York: Prentice Hall, 1990.
26. B. Etkin, *Dynamics of Flight: Stability and Control,* New York: Wiley, 1982.
27. U.S. Air Force, *MIL-STD-1797A: Flying Qualities of Piloted Aircraft,* Washington, DC: Government Printing Office 1991.
28. M. W. Spong and M. Vidyasagar, *Robot Dynamics and Control,* New York: Wiley, 1989.
29. J. J. E. Slotine and W. Li, *Applied Nonlinear Control,* Englewood Cliffs, NJ: Prentice Hall, 1991.
30. P. E. Crouch, Spacecraft attitude control and stabilization: applications of geometric control theory to rigid body models, *IEEE Trans. Auto Contr,* **29** (4): 321–331, 1984.
31. D. Aeyels, Stabilization by smooth feedback of the angular velocity of a rigid body, *Syst. Contr. Lett.,* **6** (1): 59–63, 1985.
32. H. Krishnan, M. Reyhanoglu, and H. McClamroch, Attitude stabilization of a rigid spacecraft using two control torques: a nonlinear control approach based on the spacecraft attitude dynamics, *Automatica,* **30** (6): 1023–1027, 1994.
33. P. Tsiotras, M. Corless, and M. Longuski, A novel approach for the attitude control of an axisymmetric spacecraft subject to two control torques, *Automatica,* **31** (8): 1099–1112, 1995.
34. D. C. Hyland, J. L. Junkins, and R. W. Longman, Active control technology for large space structures, *J. Guid., Contr., Dynam.,* **16** (5): 801–821, 1993.
35. S. A. Singh, Robust nonlinear attitude control of flexible spacecraft, *IEEE Trans. Aerospace Electron. Syst.,* **23** (2): 380–387, 1987.

Reading List

T. R. Kane and D. A. Levinson, *Theory and Applications.* New York: McGraw-Hill, 1985. The basic equations for rigid-body dynamics.

Special issue on attitude representations, *J. Astronaut. Sci.,* **41** (4): 1993. An exhaustive presentation of different attitude representations.

M. L. Curtis, *Matrix Groups.* New York: Springer-Verlag, 1979. A mathematical treatment of attitude motion, along with connections with group theory and Lie algebraic concepts.

F. P. J. Rimrott, *Introductory Attitude Dynamics.* New York: Springer-Verlag, 1989. Complete treatment of the dynamics of spacecraft with momentum wheels.

P. C. Hughes, *Spacecraft Attitude Dynamics.* New York: Wiley, 1986. Classic reference. Complete analysis of stability problems for single and dual-spin spacecraft.

D. L. Mingori, Effects of energy dissipation on the attitude stability of dual-spin satellites, *AIAA J.* **7**: 20–27, 1969. More on the dynamics of dual spin.

R. J. Kinsey, D. L. Mingori, and R. H. Rand, Nonlinear control of dual-spin spacecraft during despin through precession phase lock, *J. Guid., Contr., Dynam.,* **19** (1): 60–67, 1996.

J. T. Wen and K. Kreutz-Delgado, The attitude control problem, *IEEE Trans. Auto. Contr.* **36** (10): 1148–1162, 1991. Theoretical analysis of attitude control.

D. McRuer, I. Ashkenas, and D. Graham, *Aircraft Dynamics and Automatic Control.* Princeton, NJ: Princeton University Press, 1973.

J. Roskam, *Flight Dynamics of Rigid and Elastic Airplanes.* Kansas: University of Kansas Press, 1972.

Special issue on aircraft flight control, *Int. J. Contr.,* **59** (1): 1994. Recent advances in aircraft control.

R. M. Murray, Z. Li, and S. S. Sastry, *A Mathematical Introduction to Robotic Manipulation.* Boca Raton, FL: CRC Press, 1994. Mathematical treatment of attitude dynamics, rotation matrices.

T. I. Fossen, *Guidance and Control of Ocean Vehicles.* New York: Wiley, 1994. Attitude-control applications to marine vehicles.

PANAGIOTIS TSIOTRAS
University of Virginia

AUDIO, MULTIMEDIA. See MULTIMEDIA AUDIO.
AUDITING. See ACCOUNTING.
AUTHENTICATION. See CRYPTOGRAPHY; DATA SECURITY.
AUTHENTICATION SYSTEMS. See FINGERPRINT IDENTIFICATION.